THE JOURNAL OF PHYSICAL CHEMISTRY A LETTERS

2009, *113,* 6544–6547
Published on Web 05/20/2009

Dissecting Enthalpic and Entropic Barriers to Ultrafast Equilibrium Isomerization of a Flexible Molecule Using 2DIR Chemical Exchange Spectroscopy

Jessica M. Anna, Matthew R. Ross, and Kevin J. Kubarych*

Department of Chemistry, University of Michigan, 930 North University Avenue, Ann Arbor, Michigan 48109

Received: April 3, 2009; Revised Manuscript Received: May 8, 2009

Ultrafast 2DIR chemical exchange spectroscopy was used to study the dynamic equilibrium between different isomers of dicobalt octacarbonyl. Exchange of population between bridged and unbridged isomers takes place on the time scale of a few picoseconds, corresponding to activation barriers of several kcal/mol. Despite overlapping spectral features in the 2DIR spectrum, the exchange component of the waiting time dependence was isolated by exploiting the well-characterized coherent modulation of nonexchange crosspeaks. The temperature dependence of the forward and reverse rate constants enabled extraction of isomerization energy barriers, where analysis using the Eyring equation indicated a substantial entropic contribution to the free energy barrier ($\Delta S^{\ddagger}_{exp} > 0$). Comparison to quantum chemical calculations showed reasonable enthalpy agreement, but qualitative disagreement for the entropy of the transition state relative to the isomers ($\Delta S^{\ddagger}_{comp} < 0$).

The equilibrium between two species is a dynamical process where reactants are consumed at the same rate they are regenerated. Despite the ubiquity of chemical equilibria, only with the development of ultrafast chemical exchange spectroscopy has it become possible to probe equilibrium kinetics of low-barrier reactions directly in the time domain.[1−8] Dicobalt octacarbonyl [$Co_2(CO)_8$, DCO] is known to be an important catalyst and precursor to catalysts of chemical reactions including the hydroformylation[9] and Pauson−Khand reactions.[10] DCO, a flexible molecule, exists as three isomers[11] (Figure 1) at room temperature, and thus is an ideal model system to track with ultrafast exchange spectroscopy. Previous theoretical studies have explored both relative stabilities and isomerization barriers of DCO.[12,13] Using 2DIR exchange spectroscopy, we have directly observed interconversion between two of the three isomers, providing an experimental measure of the isomerization barrier. 2DIR exchange spectroscopy has been applied to systems involving two different species such as solvent−solute complexes,[2] free solute rotation about a carbon−carbon single bond,[4] hydrogen bond formation,[1,3] and fluxionality.[7] Unlike these previous studies, all three isomers of DCO have multiple overlapping vibrational transitions that complicate the isolation of the exchange component. We demonstrate a method that exploits predictable coherent quantum mechanical modulations of certain crosspeaks in the 2DIR spectrum to isolate the exchange signal, while extending chemical exchange to a system with more than two equilibrium species. By analyzing the kinetics using Arrhenius and Eyring approaches, we find a substantial entropic contribution to the reaction barrier.

2DIR spectroscopy reveals information hidden in a congested linear spectrum by spreading it over two axes.[14,15] Each excitation frequency ω_{excite} is correlated with each detection frequency ω_{detect} for a given value of the waiting time t_2 between excitation and detection. The picosecond equilibrium exchange of population between spectroscopically distinct isomers is manifested as crosspeak growths corresponding to excitation

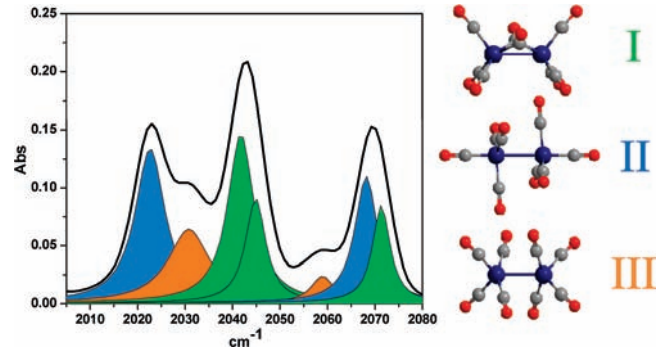

Figure 1. FT-IR spectrum of $Co_2(CO)_8$ in *n*-hexane is shown. The peaks in green at 2040, 2044, and 2070 cm^{-1} are assigned to isomer I (C_{2v}). The peaks in blue at 2022 and 2067 cm^{-1} are assigned to isomer II (D_{3d}), and the peaks in orange at 2030 and 2057 cm^{-1} are assigned to isomer III (D_{2d}).

of one isomer and detection of another isomer. A complication of 2DIR exchange spectroscopy is the possibility that an exchange peak is coincident with an ordinary crosspeak of one or more of the exchanging species. It is known, and has been studied in detail in $Mn_2(CO)_{10}$,[16] that waiting-time (t_2) coherences are an essential component of 2DIR spectra, leading to oscillations of the crosspeaks at the difference frequencies of the states comprising the coherence (i.e., off-diagonal density matrix element). In DCO such coherences produce crosspeak modulations enabling isolation of the nonexchanging signal contribution, thus extracting the exchange component.

Experiment

Our chirped-pulse upconversion detection method of Fourier transform 2DIR has been previously described in detail (see also Supporting Information).[16−18] A 130 μm thick sample of filtered 8 mM DCO in *n*-hexane was used for the 2DIR experiments. Waiting time dependent 2DIR spectra were

10.1021/jp903112c CCC: $40.75

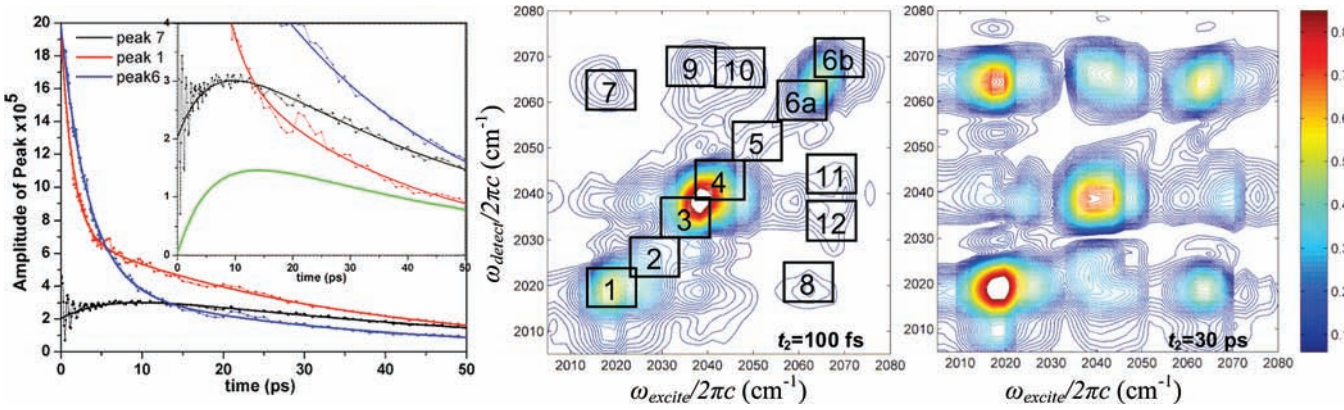

Figure 2. Plot of the amplitudes of peaks 1, 6, and 7 as a function of t_2. The inset shows the data focusing on the crosspeak along with the exchange part of the signal in green, which was obtained from the described fitting procedure. Absolute value of the rephasing spectra of $Co_2(CO)_8$ in *n*-hexane at $t_2 = 100$ fs and $t_2 = 30$ ps are shown with the spectra normalized to the maximum amplitude.

recorded over 50 ps in 100 fs steps for the first 5 ps, 250 fs steps for 5.25−10 ps, 500 fs steps for 10.5−15 ps, and 1 ps steps for the remaining 35 ps. FT-IR spectra were measured at temperatures ranging between 19 and 50 °C using a sample of 8 mM solution of DCO in *n*-hexane.

Results

Thermodynamics. The FT-IR spectrum of DCO in *n*-hexane at 25 °C is shown in Figure 1. The peaks have been previously assigned to isomer I (2040, 2044, and 2070 cm^{-1}), isomer II (2022 and 2067 cm^{-1}), and isomer III (2030 and 2057 cm^{-1}). Since exchange crosspeaks grow with a rate constant that is the sum of the forward and reverse rate constants, the equilibrium constant is needed to find the separate rate constants. The ratio of the areas of isomer I and II yields equilibrium constants at 14, 25, and 50 °C of $K_{I/II} = 1.13$, 1.09, and 1.03, respectively. From the temperature-dependent equilibrium constants, a van't Hoff plot (Supporting Information) gives $\Delta H^\circ_{II\rightarrow I} = -0.49$ kcal/mol and $\Delta S^\circ_{II\rightarrow I} = -1.46$ cal/(mol·K). At 25 °C, $\Delta G^\circ_{II\rightarrow I} = -0.053$ kcal/mol.

2DIR Experiments: Kinetics. Absolute value rephasing spectra for two different waiting times, t_2, are displayed in Figure 2. The peaks on the diagonal ($\omega_{excite} = \omega_{detect}$) are due to the fundamental transitions seen in the linear spectrum. Crosspeaks present at $t_2 = 0$ indicate that the corresponding diagonal peaks share a common ground state and thus belong to the same isomer. In accord with earlier work,[11] peak 1 is assigned to isomer II, peaks 2 and 5 are assigned to isomer III, and peaks 3 and 4 are assigned to isomer I. Both isomer II and I contribute to peak 6 with isomer II lying at lower wavenumber (6a) and isomer I at higher wavenumber (6b). The composition of peak 6 has been confirmed by temperature-dependent FT-IR spectra (Supporting Information). Crosspeaks 9, 10, 11, and 12 confirm the assignment of the diagonal peaks 3, 4, and 6b to isomer I, while the crosspeaks 7 and 8 confirm the assignment of the diagonal peaks 1 and 6a to isomer II.

The peaks in the 2D spectrum change in magnitude with increased waiting time. Figure 2 shows the amplitudes of peaks 1, 6, and 7 as a function of t_2. Peak 7 is present at $t_2 = 0$ and markedly increases in amplitude by $t_2 = 30$ ps, whereas the diagonal peaks simply decay. Biexponential fits of the diagonal peaks indicate a fast decay of 2−3 ps (1/*e*) and a slower decay of 30 ps. Crosspeak 7 first oscillates as it grows in and then decays; a Fourier transform of the crosspeak 7 oscillations yields a frequency of 46 cm^{-1}, which equals the splitting between transitions 6a and 1 of isomer II, indicating an excited state coherence of isomer II.[16] Figure 3 shows peak 7 traces taken from 2D spectra recorded at 14, 25, and 50 °C with both simple growth-decay fits as well as the component due primarily to exchange extracted following the procedure described below.

Discussion

The key challenge in extracting the exchange component from peak 7 is to remove the crosspeak contribution due to isomer II. At $t_2 = 0$, before any exchange can occur, crosspeak 7 must be due solely to isomer II. Besides exchange, an alternative origin of the growth of peak 7 is intramolecular vibrational redistribution (IVR) of population between the two modes of isomer II. The oscillating coherence is a delicate quantum mechanical condition easily disrupted by environmental fluctuations. The exchange processes itself acts as a dephasing mechanism: since once exchange occurs, the two states involved in the coherence are no longer eigenstates.[3] We therefore take the presence of the coherence to indicate *nonexchange*—that is, the coherence is due to molecules that never exchange during t_2. Removing the coherence from the total crosspeak amplitude leaves the part of the signal that is due primarily to exchange. We have focused on peak 7 because the time dependence can be modeled by accounting for the contribution of the exchange peak and a single nonexchange crosspeak; peaks 1, 3, 4, and 8 require less straightforward modeling due to multiple overlapping contributions. A diagrammatic derivation of the t_2-dependence of a nonexchange crosspeak and its removal from the measured data is given in the Supporting Information.

From our fitting procedure we obtain a rate constant of $k_f = 0.077 \pm 0.007$ ps^{-1} ($1/k_f = 13 \pm 1$ ps) for isomer II to interconvert to isomer I at 25 °C. Using the equilibrium constant obtained from FT-IR spectra ($K_{eq} = 1.09$), we obtain a reverse rate constant of $k_r = 0.071 \pm 0.007$ ps^{-1} (14 ± 1 ps) for I-to-II interconversion. Fitting data from 2D spectra taken at 14 and 50 °C results in rate constants of $k_f = 0.047 \pm 0.004$ ps^{-1} (21 ± 2 ps) and $k_f = 0.139 \pm 0.021$ ps^{-1} (7.0 ± 1 ps) for II-to-I. Reverse rate constants were determined to be $k_r = 0.042 \pm 0.004$ ps^{-1} (24 ± 2 ps) and $k_r = 0.135 \pm 0.021$ ps^{-1} (7 ± 1 ps). Direct comparison of k_f to k_r shows that II-to-I interconversion is more rapid than I-to-II interconversion, consistent with a negative $\Delta G^\circ_{II\rightarrow I}$.

To establish further evidence for the assignment of an exchange component in peak 7, we considered the difference in the temperature dependence of the diagonal and crosspeaks. Previous studies of IVR in metal carbonyls observed crosspeak growth with a rate constant similar to the fast decay of the

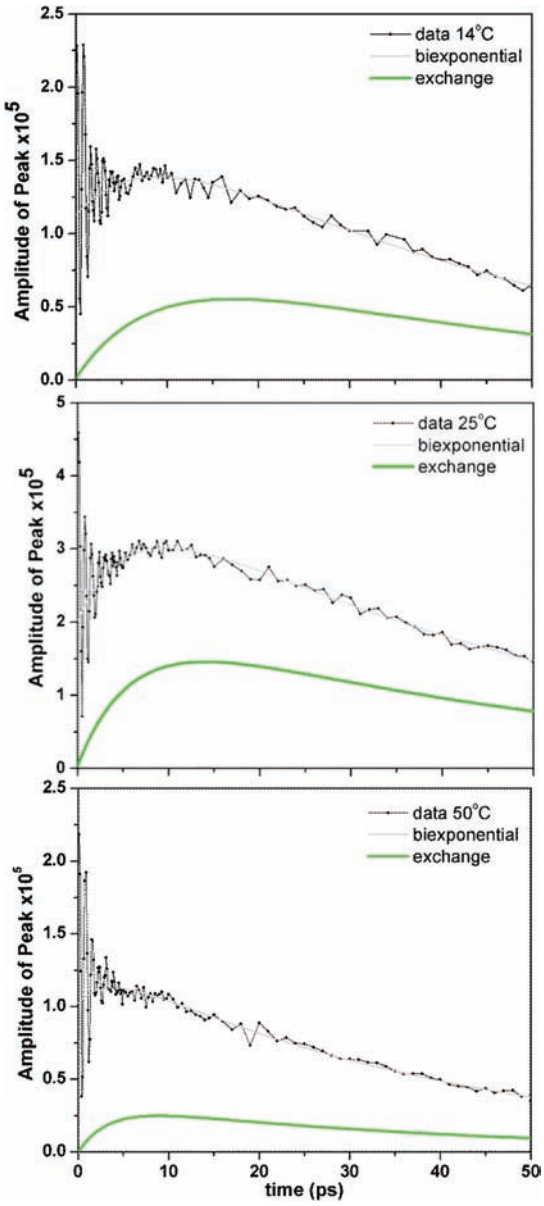

Figure 3. Waiting time dependent traces of peak 7 at 14, 25, and 50 °C shown with (solid black) a simple biexponential fit accounting for growth and decay and (green) the isolated exchange component.

corresponding diagonal peaks.[19] In order for growth of peak 7 to be due to IVR among the eigenstates of isomer II—both bright and dark—the growth of the crosspeak and IVR decay of the diagonal peaks should have the same temperature dependence, but this is not observed (Supporting Information). This assignment is further justified since the two isomer-II normal modes whose coupling leads to peak 7 involve different local carbonyl units.[7] Thus we assign the growth of peak 7 to chemical exchange between isomer II and isomer I.

An Arrhenius plot (Figure 4a) yields an activation energy for II-to-I of $E_a = 5.4$ kcal/mol and for I-to-II, $E_a = 5.8$ kcal/mol. This value is similar to other ultrafast chemical exchange measurements of similar time scale processes, though the barrier observed here is larger than that measured for fluxional pseudorotation in $Fe(CO)_5$,[7] consistent with the larger structural deformation in DCO. The Arrhenius plot does not take into account the temperature dependence of the solvent's viscosity. Over the temperature range of interest, the activation barrier due to the viscosity for *n*-hexane is estimated to be $E_a^{\eta} = 1.6$ kcal/mol (see Supporting Information), reducing the barrier to $E_a - E_a^{\eta} = 3.8$ kcal/mol for II-to-I and $E_a - E_a^{\eta} = 4.2$ kcal/mol for I-to-II. E_a provides an upper limit while $E_a - E_a^{\eta}$ provides a lower limit to the enthalpic barrier to isomerization, $\Delta H^{\ddagger}$.[20] Since isomerization induces a significant structural change between bridged and unbridged isomers, we also considered the entropic contribution to the energy barrier for isomerization (Figure 4a). Eyring plots yield $\Delta H^{\ddagger} = 4.8$ kcal/mol and $\Delta S^{\ddagger} = 7.2$ cal/(mol·K) (1.2 kcal/mol at 298 K) for II-to-I interconversion and $\Delta H^{\ddagger} = 5.2$ kcal/mol and $\Delta S^{\ddagger} = 8.4$ cal/(mol·K) (2.7 kcal/mol at 298 K) for I-to-II. Assuming for simplicity ideal Kramers behavior in the high friction limit, we can include the temperature dependence of the viscosity in the rate constant (eq 1).[20] The Stokes−Einstein equation for friction with slip boundary conditions was used and I is the moment of inertia, ω_b is the frequency of the barrier, d is the hydrodynamic radius, and r is the radius of gyration of the moving group.

$$k = \omega_b \left(\frac{I}{4\pi\eta_o d r^2}\right)\left(\frac{k_b T}{h}\right) e^{-E_a^{\eta}/RT} e^{\Delta S/R} e^{-E_a/RT} \qquad (1)$$

An explanation on how these parameters were obtained is given in the Supporting Information. Using eq 1, we extracted $\Delta S^{\ddagger} = 1.57$ cal/(mol·K) from the intercept and $\Delta H^{\ddagger} = 3.18$ kcal/mol from the slope of the Eyring plot for II-to-I interconversion; for I-to-II, $\Delta S^{\ddagger} = 2.82$ cal/(mol·K) and $\Delta H^{\ddagger} = 3.60$ kcal/mol. From these values $\Delta G^{\ddagger}$ at 298 K was calculated to be 2.72 kcal/mol for II-to-I and 2.76 kcal/mol for I-to-II interconversion. Given the substantial entropic contribution, the Eyring analysis indicates that the Arrhenius assumption of an isentropic, solvent viscosity independent reaction may be unwarranted (Figure 4b).

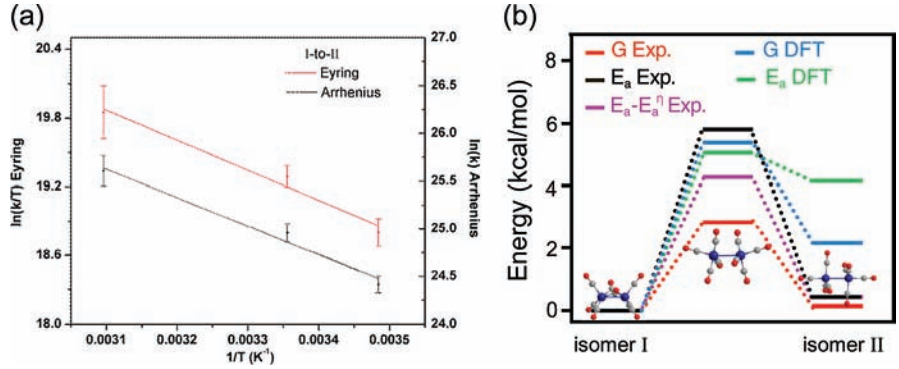

Figure 4. (a) Kinetic analysis of the I-to-II isomerization using Arrhenius and Eyring methods (solid lines are linear fits). (b) Summary of experimental and computationally determined energies of the two isomers and the transition state.

Using the GAMESS package,[21] DFT calculations were carried out on isomer I, isomer II, and the corresponding transition state for interconversion. Previous computational studies of DCO using DFT with the B3LYP functional found isomer I to be lower in energy than isomer II.[12,13] Experimentally, we have observed the direct isomerization between isomer I and II, as well as finding isomer I to lie lower in energy. Using B3LYP/6-31G(2df), the transition state was found and the barrier for I-to-II interconversion was determined to be $E_a = 5.26$ kcal/mol and $E_a = 1.05$ kcal/mol for II-to-I. The relative energies of the isomers are consistent with the previous computational studies using B3LYP,[12,13] and for the I-to-II barrier, the agreement with experiment is surprisingly good (Figure 4b). Although $\Delta S^{\ddagger}$ is found experimentally to play a role in determining the overall isomerization barrier, the DFT results found that $\Delta S^{\ddagger}$ does not have a large effect on computed barriers (Figure 4b). Comparing computed and experimentally determined $\Delta S^{\ddagger}$, we find $\Delta S^{\ddagger}_{exp} > 0$ while $\Delta S^{\ddagger}_{comp} < 0$. Though an isolated-molecule calculation cannot be expected to agree with a solution phase experiment, the reasonable enthalpy agreement suggests the solvent influences primarily the entropy of the molecules, perhaps by entropically stabilizing the two isomers relative to the transition state. Current work is underway to investigate the effects of solvent viscosity on the equilibrium exchange kinetics.

Conclusion

2DIR spectroscopy has enabled a probe of the ultrafast equilibrium exchange between isomers of $Co_2(CO)_8$. Using the coherent modulation of crosspeaks as an indicator of nonexchange, we have demonstrated that even in systems with complex multilevel vibrational structure it is possible to isolate the chemical exchange signature. Temperature dependent studies enabled separation of IVR from chemical exchange processes while yielding the activation barrier, E_a, and $\Delta G^{\ddagger}$ for equilibrium isomerization. Comparison of Arrhenius and Eyring analysis shows that the entropy makes a substantial contribution to the energy barriers for isomerization, most likely due to the large structural changes associated with switching between bridging and nonbridging forms. Comparison of experimental data to DFT calculations suggests that the solvent has a large effect on the relative free energies of the isomers, and further studies will explore the effects of solvent on equilibrium kinetics and thermodynamics.

Acknowledgment. This work was supported by the NSF (CHE-0748501) and the ACS Petroleum Research Fund.

Supporting Information Available: Derivation of coherence t_2 dependence, example of the fitting procedure, temperature dependent FT-IR, biexponential fit, Fourier transform of coherence oscillations, Arrhenius and Eyring plots, thermodynamic properties, temperature dependence of decays, and calculated structures. This material is available free of charge via the Internet at http://pubs.acs.org.

References and Notes

(1) Woutersen, S.; Mu, Y.; Stock, G.; Hamm, P. *Chem. Phys.* **2001**, *266*, 137–147.
(2) Zheng, J. R.; Kwak, K.; Asbury, J.; Chen, X.; Piletic, I. R.; Fayer, M. D. *Science* **2005**, *309*, 1338–1343.
(3) Kim, Y. S.; Hochstrasser, R. M *Proc. Natl. Acad. Sci. U.S.A.* **2005**, *102*, 11185–11190.
(4) Zheng, J. R.; Kwak, K. W.; Xie, J.; Fayer, M. D. *Science* **2006**, *313*, 1951–1955.
(5) Ishikawa, H.; Kwak, K; Chung, J. K.; Kim, S.; Fayer, M. D *Proc. Natl. Acad. Sci. U.S.A.* **2008**, *105*, 8619–8624.
(6) Kim, Y. S.; Hochstrasser, R. M. *J. Phys. Chem. B* **2007**, *111*, 9697–9701.
(7) Cahoon, J. F.; Sawyer, K. R.; Schlegel, J. P.; Harris, C. B. *Science* **2008**, *319*, 1820–1823.
(8) Kim, Y. S.; Liu, L.; Axelsen, P. H.; Hochstrasser, R. M *Proc. Natl. Acad. Sci. U.S.A.* **2008**, *105*, 7720–7725.
(9) Tannenbaum, R.; Bor, G. *J. Organomet. Chem.* **1999**, *586*, 18–22.
(10) Chung, Y. K. *Coord. Chem. Rev.* **1999**, *188*, 297–341.
(11) Sweany, R. L.; Brown, T. L. *Inorg. Chem.* **1977**, *17*, 415–421.
(12) Kenny, J. P.; King, R. B.; Schaefer, H. F. *Inorg. Chem.* **2001**, *40*, 900–911.
(13) Aullón, G.; Alvarez, S. *Eur. J. Inorg. Chem.* **2001**, *2001*, 3031–3038.
(14) Jonas, D. M. *Annu. Rev. Phys. Chem.* **2003**, *54*, 425–463.
(15) Cho, M. H. *Chem. Rev.* **2008**, *108*, 1331–1418.
(16) Nee, M. J.; Baiz, C. R.; Anna, J. M.; McCanne, R.; Kubarych, K. J. *J. Chem. Phys.* **2008**, *129*, 084503.
(17) Nee, M. J.; McCanne, R.; Kubarych, K. J.; Joffre, M. *Opt. Lett.* **2007**, *32*, 713–715.
(18) Baiz, C. R.; Nee, M. J.; McCanne, R.; Kubarych, K. J. *Opt. Lett.* **2008**, *33*, 2533–2535.
(19) Khalil, M.; Demirdoven, N.; Tokmakoff, A. *J. Chem. Phys.* **2004**, *121*, 362–373.
(20) Flom, S. R.; Nagarajan, V.; Barbara, P. F. *J. Phys. Chem.* **1986**, *90*, 2085–2092.
(21) Schmidt, M. W.; Baldridge, K. K.; Boatz, J. A.; Elbert, S. T.; Gordon, M. S.; Jensen, J. H.; Koseki, S.; Matsunaga, N.; Nguyen, K. A.; Su, S. J.; Windus, T. L.; Dupuis, M.; Montgomery, J. A. *J. Comput. Chem.* **1993**, *14*, 1347–1363.

JP903112C